Study on the Transmission Characteristics of Symmetric Hybrid Long-range Surface Plasmon Polariton Waveguide

Zhang Guanmao Sun Haili Li Jianming Zhao Hai

(*Institute of Modern Communication Technology, School of Information Science and Engineering, Lanzhou University, Lanzhou, Gansu* 730000, *China*)

Abstract A novel symmetric hybrid long-range surface plasmon polariton waveguide structure is proposed and numerically analyzed. The results show that the proposed structure provides a better trade-off between the propagation length and mode confinement. The characteristics of the mode effective index, mode width, propagation length and figures of merit of the fundamental mode supported by this waveguide structure are calculated at the telecom wavelength 1550 nm for different dimensions of the polymer ridge and relatively low index dielectric regions (RLIDRs) under the metal. It is shown that the symmetric structure exhibits an increase in the propagation length, as well as a substantial increase in the figures of merit at the maximum point of the propagation length. For these advantages, the symmetric hybrid long-range surface plasmon polariton waveguide is a good candidate for realizing highly functional density photonic integration circuits.

Key words integrated optics; symmetric hybrid long-range surface plasmon polariton waveguide; finite element method; propagation length; mode width; figure of merit

OCIS codes 130.3120; 130.2790; 130.5460

一种对称混合长程表面等离子激元波导传输特性研究

张冠茂 孙海丽 李建明 赵 海

(兰州大学信息科学与工程学院 现代通信技术研究所, 甘肃 兰州 730000)

摘要 提出一种新颖的对称混合长程表面等离子激元波导结构并对其进行了数值分析。结果表明在传播长度与模式限制两个特性之间实现了很好的平衡。在通信波长 1550 nm 处,利用有限元数值仿真方法分析了该结构在不同介质尺寸下基模的有效折射率、模式宽度、传播长度和品质因数。计算结果表明:对称混合长程表面等离子激元波导的传播长度及传播长度最大值点的品质因数都有明显的提高。鉴于这些优点,该对称混合长程表面等离子激元波导在实现高性能、高密度的光子集成电路方面具有一定的潜在用途。

关键词 集成光学; 对称混合长程表面等离子激元波导; 有限元法; 传播长度; 模式宽度; 品质因数

中图分类号 O43 **文献标识码** A **doi**: 10.3788/LOP50.121301

1 Introduction

Future photonic integrated circuits for the optical information will have special requirements on the density of integration[1-2]. Surface plasmon polaritons (SPPs), which are the surface electromagnetic waves strongly restricted to the metal-dielectric interface, have the distinct ability to centralize and guide light in subwavelength scale[3-5]. As a consequence, the waveguide based on the SPPs shows full prospect for the applications in the highly photonic integrated devices. It has been widely researched recently[6], such as metallic nano-wires[7-8], nano-stripes[9], channel SPP waveguides (rectangle grooves and V-shaped grooves)[10] and wedges[11]. However, a noticeable point is the existing trade-off between the field confinement and the propagation length.

Long-range surface plasmon polariton (LRSPP) waveguide plays an importance role for its long propagation length

收稿日期: 2013-07-29; **收到修改稿日期**: 2013-09-12; **网络出版日期**: 2013-11-12

基金项目: 中央高校基本科研业务费专项资金(兰州大学)(lzujbky-2012-40)

作者简介: 张冠茂(1973—),男,博士,副教授,主要从事光通信、光传感、微纳光子晶体以及光域表面等离子体激元共振理论与应用。E-mail: zhanggm@lzu.edu.cn

at the telecom wavelength 1550 nm[12]. However, the field confinement of the LRSPP waveguide is very weak. In order to reduce the mode size and get higher densities of integration, the dielectric loaded surface plasmon polariton (DLSPP) waveguide with strong field confinement was proposed and demonstrated[13-15]. Nevertheless, the propagation length of the DLSPP waveguide decreases significantly compared with the LRSPP waveguide mode because the proportion of the electromagnetic field distributed in the lossy metal film increased greatly. In order to further improve the propagation length and reduce the mode size, the symmetric dielectric loaded surface plasmon polarition (SDLSPP) waveguide, which supports a symmetric mode propagation within the high index dielectric ridges surrounded by the low index dielectric layer and combines both the advantages of LRSPP and DLSPP waveguides, has been presented[16-17]. However, the transmission loss is still remarkable since the proportion of the electromagnetic fields increases in the lossy metal film. Recently, reports indicated that by adding thin dielectric layers with low index at the metal surface to form the core and inserting it into the high index dielectric layer, which is called the hybrid long-range surface plasmon polariton (HLRSPP) waveguide, can effectively reduce the field concentration in the metal film. It leads to a great increase in the propagation length[18-19]. Such a waveguide structure comprises two relatively low index dielectric regions (RLIDRs) symmetrically distributed on both sides of a narrow metal stripe. The field confinement in the horizontal and vertical directions could be obtained with a low transmission loss[20]. Moreover, the RLIDRs are used to guide and confine light in the sub-wavelength optics ascribed to the slot waveguide[21].

In this paper, a novel symmetric hybrid dielectric-metal-dielectric waveguide structure is proposed to support HLRSPP propagation. We draw into an increase of the propagation length and a highly confined mode field for HLRSPP waveguide by adding the upper cladding symmetric with substrate. It can form a symmetric three-dielectric-layer stack with a low-high-low dielectric constant distribution with strong confinement and low propagation loss. So it can lead to an increase in the propagation length and thus the increase in figures of merit as well for the superposition of electromagnetic fields in metal-dielectric interface in this symmetric waveguide structure. All the simulations in this paper are performed by using rigorous numerical schemes based on finite element method (FEM) at the telecom wavelength.

2 Fundamental mode characteristics

The proposed symmetric HLRSPP waveguide structure is shown in Fig. 1. The narrow gold stripe (with 20 nm thickness and 350 nm width, $n_1 = 0.55 + 11.5\mathrm{i}$[22]) is located in the middle of the high index dielectric ridges ($n_3 = 2.0$[22]) and the two RLIDRs ($n_2 = 1.34$) with the same size are symmetrically loaded on each side of the metal stripe, which is supported by a poly-methyl methacrylate (PMMA) substrate with the index $n_4 = 1.49$. An upper cladding ($n_4 = 1.49$) is deposited on the top of the dielectric ridges. The surrounding of the waveguide is air.

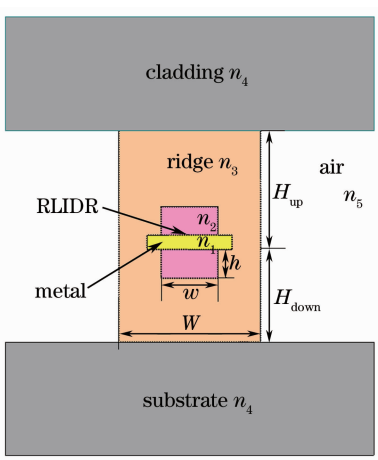

Fig. 1 Cross-section of the symmetric HLRSPP waveguide structure. $W = 600$ nm, $w = 200$ nm, $H_{up} = 500$ nm

2.1 Mode effective index and normalized attenuation constant

In general, the complex propagation constant is written as

$$k_{spp} = k'_{spp} + \mathrm{i}k''_{spp}. \tag{1}$$

The normalized propagation constant is defined as

$$\overline{k_{spp}} = \overline{k'_{spp}} + \mathrm{i}\,\overline{k''_{spp}} = \frac{k'_{spp} + \mathrm{i}k''_{spp}}{k_0} = \frac{\beta + \mathrm{i}\alpha}{k_0}. \tag{2}$$

For a metal surface, the SPPs normalized propagation constant is $N_{eff} = \beta/k_0 + \mathrm{i}\alpha/k_0$, where $k_0 = 2\pi/\lambda_0$ is the wave

number and λ_0 is the wavelength in free space. Re(N_{eff}) is the mode effective index, Im(N_{eff}) is the normalized attenuation constant[15]. The dependences of the mode effective index and the normalized attenuation constant on different dielectric RLIDR dimensions h under the metal are found by FEM. Figure 2 shows that the mode effective index decreases with the increase of the dielectric RLIDR height h under the metal, and the normalized attenuation constant reaches the minimum when h = 395 nm and then increases.

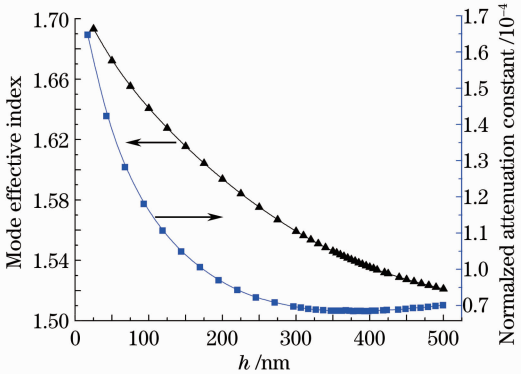

Fig. 2 Mode effective index and normalized attenuation constant versus the heighth of RLIDR under the metal (H_{down} = 510 nm)

In contrast with the trend of RLIDR height, the influence of different dimensions on the hybrid LRSPP waveguide mode of the proposed structure (mode effective index and normalized attenuation constant) is investigated and the results are shown in Fig. 3. In this simulation, increasing the dielectric ridge height H_{down} under the metal can lead to the increase of mode effective index. The mode effective index increases on account of a majority of the electromagnetic field into the high index region with H_{down} increases. Increasing the height of the dielectric ridge H_{down} has a little influence on the normalized attenuation constant. For the symmetric HLRSPP waveguide, the normalized attenuation constant can get up to the minimum at the point of H_{down} = 510 nm.

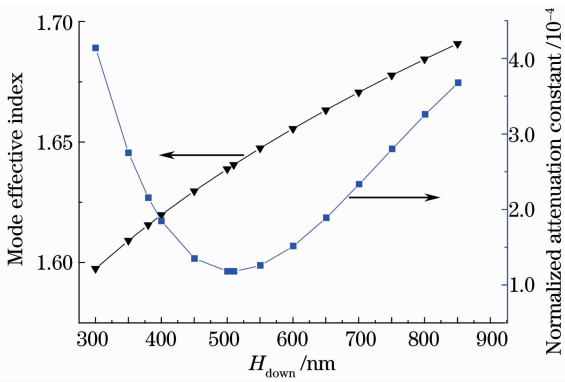

Fig. 3 Mode effective index and normalized attenuation constant versus the height of ridge H_{down} under the metal (h = 100 nm)

2.2 Propagation length

The propagation length that relies on the dielectric RLIDR height under the metal is investigated for the symmetric HLRSPP waveguide and shown in Fig. 4. The propagation length of the hybrid LRSPP waveguide mode is calculated as $L_p = \lambda_0/[4\pi\mathrm{Im}(N_{eff})]$. In contrast to the normalized attenuation constant, the propagation length of the

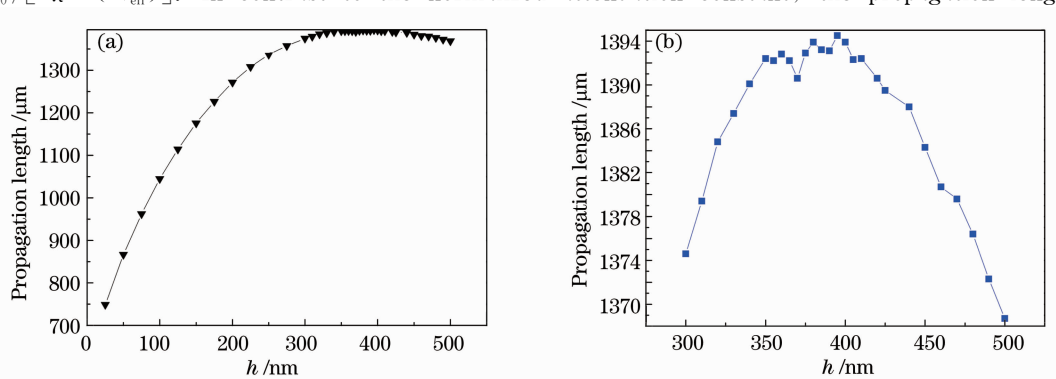

Fig. 4 Propagation length as a function of the height h of the RLIDR under the metal (H_{down} = 510 nm)

fundamental mode supported by the symmetric HLRSPP waveguide increases with the increase of the dielectric RLIDR height h in the beginning and then decreases. In order to see clearly the variation trend of the propagation length from 300 nm to 500 nm, the detailed propagation length distribution of RLIDR height under metal between 300 nm and 500 nm is shown in Fig. 4(b). In accordance with the general consideration, it is exciting that the propagation length of the fundamental mode supported by the symmetric HLRSPP waveguide is 1394 μm at the maximum point h = 395 nm. From the trend of the curve, we can see that there is a continuous oscillation region between 350 nm and 410 nm.

In industrial fabrication, the symmetric HLRSPP waveguides are fabricated by using electron-beam lithography rather than the large-scale ultraviolet (UV) lithography[23]. The fabrication of this proposed structure can be implemented by all layers deposition first, and then electron-beam lithography patterning and etching, followed by the plasma-enhanced chemical-vapor deposition of the dielectric materials and metal[24]. However, it is very difficult to fabricate the ideal dimension dielectric ridge of symmetric HLSPP waveguide in practical fabrication processing due to the fabrication errors. The propagation length of the symmetric HLRSPP waveguide moves around 1392 μm with the increase of the RLIDR height h, the tiny variation of the propagation length of the symmetric HLRSPP waveguide will not be sensitive to the fabrication errors from 350 nm to 410 nm, so the symmetric HLRSPP waveguide structure facilitates manufacturing.

The propagation length of the fundamental mode of the symmetric HLRSPP waveguide as a function of the ridge height H_{down} for the configuration is shown in Fig. 5. It looks like a parabola, and the symmetry axis of the propagation length curve is H_{down} = 510 nm. It seems to have a maximum of 1045 μm at the ridge height of H_{down} = 510 nm approximately. In accordance with the general consideration, it is exciting that the propagation length of the fundamental mode supported by the cladding HLRSPP waveguide is longer than that supported by the non-cladding HLRSPP waveguide when the dielectric ridge height H_{down} > 450 nm. From Fig. 5, we can see that the propagation length of the cladding HLRSPP waveguide is 1045 μm at H_{down} = 510 nm, while the propagation length of the non-cladding HLRSPP waveguide is 845 μm at H_{down} = 380 nm. This cladding structure exhibits an increase of almost 24% in the propagation distance. The inset of Fig. 5 shows the distribution of the normalized electric field distribution of the fundamental mode for the proposed symmetric HLRSPP waveguide when H_{down} = 510 nm.

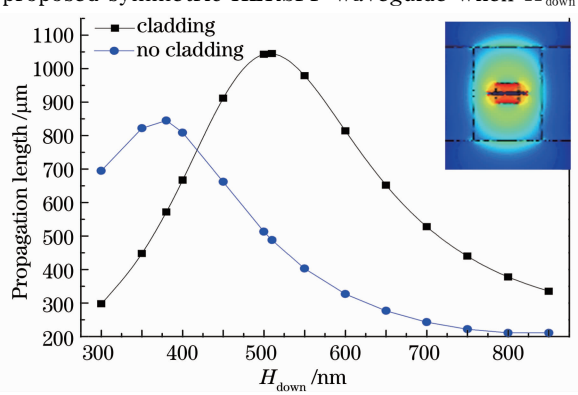

Fig. 5 Comparison of the propagation length versus H_{down} under the metal for the cladding and non-cladding structures (h = 100 nm)

3 Lateral mode field confinement

In the design of photonic integration components, the lateral mode field confinement gets much more concern, because of a good confinement, i.e., a small mode width. This characteristic not only enables large density of devices to reduce the consequent propagation loss[12], but also plays an important role when realizing both passive and active components, as it is the lateral mode width which determines the minimum achievable bend radius without introducing large bending losses. The lateral mode width is found by taking the width of the norm of the electric field at 1/e of its maximum value, as described more detailedly in Ref. [25].

In order to find the mode width of the fundamental mode for different heights h of the dielectric RLIDR under the metal, the field profiles of the lateral cross section should be taken into account. The typical profiles of the fundamental mode of the symmetric waveguide structure are revealed in Fig. 6. The mode width increases monotonically with the increase of the height h of the ridge under the metal in Fig. 6(a). In contrast with h, Fig. 6(b) has a contrary trend.

Corresponding to typical values commonly used by the other authors to satisfy the requirements of the highly integrated photonic devices needing both tight mode field confinement and long propagation length, Fig. 6(c) shows the simulated results of the dependence of the HLRSPP waveguide mode of the proposed structure (propagation

length and mode width) on the geometric parameter H_{down}. The results for the non-cladding structure are also provided for comparison. From the figure, it can be seen that, for the same value of mode width, the value of the propagation length of the cladding structure is longer when the mode width is less than 0.827 μm. This is the better trade-off standard between the propagation length and the mode confinement. Furthermore, the smaller mode width and the longer propagation distance can be reflected in the cladding structure.

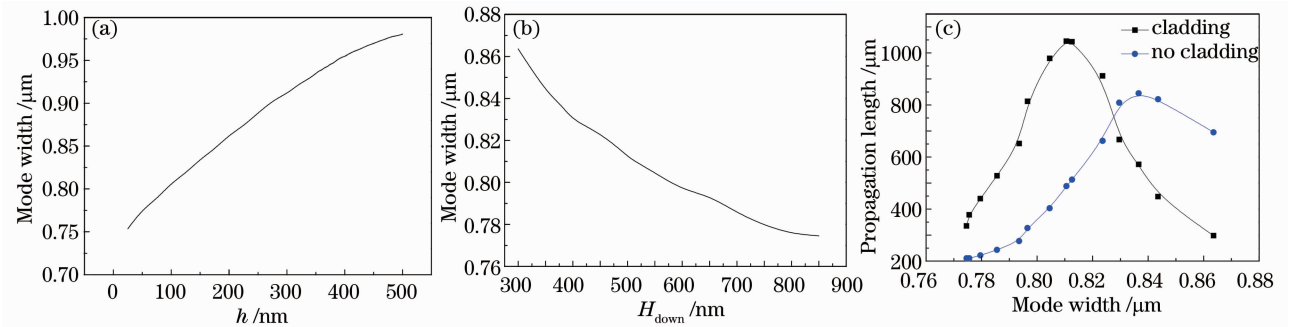

Fig. 6 Curves of mode width. (a) Mode width as a function of h (H_{down} = 510 nm); (b) mode width versus H_{down} (h = 100 nm); (c) propagation length versus mode width (h = 100 nm)

The above analysis shows that the dependence of propagation length on the parameter h is larger than H_{down}, and the dependence of mode width on the parameter h is also larger than that on H_{down}. This is the contradiction between the propagation length and mode confinement. In order to solve the problem, we recommend figures of merit parameter.

4 Figures of merit

To further assess the performance of the HLRSPP waveguides, we introduce a parameter named figure of merit (FoM), which was proposed as the quality measures for the SPP waveguides by Berini[26]. FoM is useful to optimize the dimensions of the SPP waveguides and measure the attenuation-confinement trade-off, where three FoMs are denoted as M_1, M_2 and M_3 respectively, which are defined as the "confinement-to-attenuation" ratio for a particular mode[26].

The first FoM M_1 is useful for evaluating the waveguides in applications where it is important to achieve a prescribed or small mode width, such as end-fire coupling to a source and dense optical interconnects. $M_1 = 2\sqrt{\pi}L/\sqrt{S}$, which is a ratio of propagation length to mode area[27]. The mode area S is bounded by the closed 1/e field magnitude contour relative to the global field maximum, and L is the propagation length. In general, the higher FoM M_1 is, the better the field mode is confined in RLIDRs. M_2 is useful for comparing waveguides in applications where it is important to achieve prescribed or large distance from the light line, for instance, Bragg gratings. $M_2 = L^2\lambda/W^3$, where λ is the wavelength, and W is the mode width[12]. The higher M_2 demonstrates the great potential of the considered waveguide structure. $M_3 = \mathrm{Re}(N_{eff})/2\pi\mathrm{Im}(N_{eff})$, and it is useful for comparing waveguides in applications where achieving a small guided wavelength is important, such as in the design of nano-resonators or nano-scale grating couplers[26].

The symmetric HLRSPP waveguide structure is more suitable for M_2 and M_3. It is obvious that the proposed structure features significantly higher values of $M_2 = 3.18 \times 10^6$ and $M_3 = 2210$ when H_{down} = 510 nm compared with

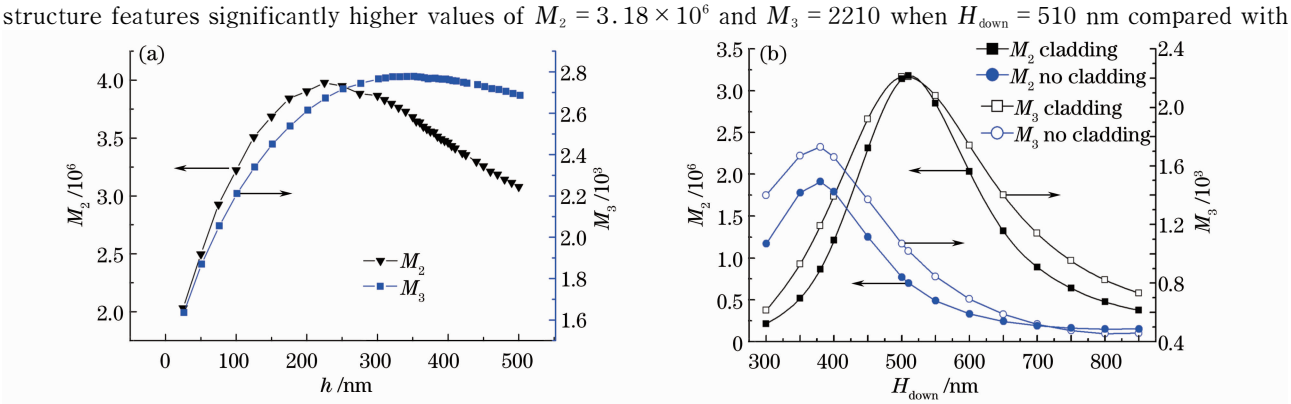

Fig. 7 Figures of merit of the fundamental mode for the HLRSPP waveguides. (a) M_2, M_3 versus h (H_{down} = 510 nm); (b) M_2, M_3 versus H_{down} (h = 100 nm)

the non-cladding structure. We can find that the maximum of the figure of merit M_2 of the cladding structure increases by 66% compared with the non-cladding structure at the maximum point of the propagation length. The figure of merit M_3 of the cladding structure increases by about 27% compared with the non-cladding structure at the maximum point of the propagation length. The maximum M_2 and M_3 are at different height h compared with the maximum point of the propagation length at h = 395 nm. For instance, the figure of merit M_2 of the symmetric structure reaches its maximum of 3.97×10^6 when h = 225 nm, and the figure of merit M_3 gets its maximum of 2777 at h = 350 nm. Thus it is demonstrated that the considered cladding structure has a great potential in the applications.

5 Conclusion

In this paper, we proposed a novel symmetric HLRSPP waveguide structure with a high degree of mode confinement and long propagation distance. Main characteristics including the mode effective index, field confinement, propagation length, and figures of merit of the novel HLRSPP waveguide were calculated at the telecom wavelength λ = 1550 nm for different heights of the dielectric ridge H_{down} and RLIDRs h under the metal. The symmetric structure was found to exhibit increase in the propagation length and a substantial increase in the figures of merit, which almost showed similar confinement as compared with the non-symmetric HLRSPP waveguide. The simulation results show that the proposed structure provides a better trade-off between the propagation length and mode confinement. For these advantages, the symmetric HLRSPP waveguide is a good sub-wavelength confinement structure, which can effectively reduce the transmission loss while keeping a sub-wavelength scale confinement. So the symmetric HLRSPP waveguide is a good candidate for realizing highly functional density photonic integration circuits.

References

1 Heinz Raether. Surface Plasmons on Smooth and Rough Surfaces and on Gratings[M]. Berlin: Springer, 1988.

2 Li Zhiquan, Gao Xiaoguang, Niu Liyong, *et al*.. Propagation properties of a surface plasmon polariton directional coupler[J]. Chinese J Lasers, 2012, 39(10): 1010001.
李志全,高晓光,牛力勇,等. 一种表面等离子体激元定向耦合器的传输特性[J]. 中国激光, 2012, 39(10): 1010001.

3 W L Barnes, A Dereux, T W Ebbesen. Surface plasmon subwavelength optics[J]. Nature, 2003, 424(6950): 824-830.

4 Zhang Yangyang, Zhu Fangming, Shen Linfang, *et al*.. Terahertz surface plasmon polaritons on metal surfaces corrugated by shallowly dielectric-filled grooves[J]. Acta Photonica Sinica, 2012, 41(4): 389-393.
张羊羊,朱方明,沈林放, 等. 介质填充浅槽周期结构表面上的太赫兹表面等离子体激元[J]. 光子学报, 2012, 41(4): 389-393.

5 Wu Pinghui, Gu Juguan, Liu Bin, *et al*.. Experimental research on wavelength modulation surface plasmon resonance sensor [J]. Laser & Optoelectronics Progress, 2012, 49(2): 022501.
吴平辉,顾菊观,刘 彬, 等. 波长检测型表面等离子体共振传感器的实验研究[J]. 激光与光电子学进展, 2012, 49(2): 022501.

6 Xiao-Yang Zhang, A Hu, J Z Wen, *et al*.. Numerical analysis of deep sub-wavelength integrated plasmonic devices based on semiconductor-insulator-metal strip waveguides[J]. Opt Express, 2010, 18(18): 18945-18959.

7 Pierre Berini. Plasmon-polariton waves guided by thin lossy metal films of finite width: bound modes of symmetric structures [J]. Phys Rev B, 2000, 61(15): 10484-10503.

8 Qin Xiaojuan, Guo Yanan, Xue Wenrui. Numerical simulation of a surface plasmonic waveguide with double parallel columniform metallic nanorods coated with gain medium[J]. Chinese J Lasers, 2011, 38(3): 0310001.
秦小娟,郭亚楠,薛文瑞. 带有增益介质包层的两个平行圆柱形纳米金属棒构成的表面等离子体光波导的数值模拟[J]. 中国激光, 2011, 38(3): 0310001.

9 J Takahara, S Yamagishi, H Taki, *et al*.. Guiding of a one-dimensional optical beam with nanometer diameter[J]. Opt Lett, 1997, 22(7): 475-477.

10 Bian Y S, Zheng Z, Zhao X, *et al*.. Hybrid plasmon polariton guiding with tight mode confinement in a V-shaped metal/dielectric groove[J]. J Opt, 2013, 15(5): 055011.

11 D F P Pile, T Ogawa, D K Gramotnev, *et al*.. Theoretical and experimental investigation of strongly localized plasmons on triangular metal wedges for subwavelength waveguiding[J]. Appl Phys Lett, 2005, 87(6): 061106.

12 J Gosciniak, T Holmgaard, S I Bozhevolnyi. Theoretical analysis of long-range dielectric-loaded surface plasmon polariton waveguides[J]. J Lightwave Technol, 2011, 29(10): 1473-1481.

13 T Holmgaard, S I Bozhevolnyi. Theoretical analysis of dielectric-loaded surface plasmon-polariton waveguides[J]. Phys Rev B, 2007, 75(24): 245405.

14 A V Krasavin, A V Zayats. Three-dimensional numerical modeling of photonic integration with dielectric-loaded SPP waveguides[J]. Phys Rev B, 2008, 78(4): 045425.

15 Zhao H, Li Y E, Zhang G M. Study on the performance of bimetallic layer dielectric-loaded surface plasmon polariton waveguides[J]. J Opt, 2011, 13(11): 115501.

16 Yun B F, Hu G H, Cui Y P. Bound modes analysis of symmetric dielectric loaded surface plasmon-polariton waveguides[J]. Opt Express, 2009, 17(5): 3610 - 3618.
17 J J Chen, Z Li, S Ye, *et al*.. Hybrid long-range surface plasmon-polariton modes with tight field confinement guided by asymmetrical waveguides[J]. Opt Express, 2009, 17(26): 23603 - 23609.
18 R Adato, J P Guo. Modification of dispersion, localization, and attenuation of thin metal stripe symmetric surface plasmon-polariton modes by thin dielectric layer[J]. J Appl Phys, 2009, 105(3): 034306 - 034317.
19 R F Oulton, V J Sorger, D A Genov, *et al*.. A hybrid plasmonic waveguide for subwavelength confinement and long-range propagation[J]. Nature Photon, 2008, 2(8): 496 - 500.
20 Sun X H, Xia L P, Du J L, *et al*.. A hybrid long-range surface plasmon waveguide comprising a narrow metal stripe surrounded by the low-index dielectric regions[J]. Opt Commun, 2012, 285(21 - 22): 4359 - 4363.
21 Q F Xu, V R Almeida, R R Panepucci, *et al*.. Experimental demonstration of guiding and confining light in nanometer-size low-refractive-index material[J]. Opt Lett, 2004, 29 (14): 1626 - 1628.
22 E D Palik. Handbook of Optical Constants of Solids (1st ed.)[M]. New York: Academic Press, 1985.
23 Dong Qiming, Guo Xiaowei. Numerical analysis of SPP maskless interference lithography system [J]. Acta Photonica Sinica, 2012, 41(5): 558 - 564.
董启明,郭小伟. 表面等离子体无掩膜干涉光刻系统的数值分析[J]. 光子学报, 2012, 41(5): 558 - 564.
24 W R Xue, Y N Guo, P Li, *et al*.. Propagation properties of a surface plasmonic waveguide with double elliptical air cores [J]. Opt Express, 2008, 16 (14): 10710 - 10720.
25 A Degiron, S Y Cho, C Harrison, *et al*.. Experimental comparison between conventional and hybrid long-range surface plasmon waveguide bends[J]. Phys Rev A, 2008, 77(2): 021804(R).
26 Pierre Berini. Figures of merit for surface plasmon waveguides[J]. Opt Express, 2006, 14(26): 13030 - 13042.
27 R Buckley, Pierre Berini. Figures of merit for 2D surface plasmon waveguides and application to metal stripes[J]. Opt Express, 2007, 15(19): 12174 - 12182

2014 慕尼黑上海光博会：工业激光市场前途无量

记者 朱俊刚

今天，由于激光加工独特的柔性和生产效率，它已经成为各个生产环节中的独特工艺，尤其是"激光金属加工"在各个工业行业已经得到广泛应用，如激光对于工业金属的焊接、打孔、切割、打标、蚀刻、微调、划线、激光热处置和外表处置等等，大大减少了材料加工的时间，提高工作效率。

而当“如何实现稳定的高效生产”这个问题被推上风头浪尖时，一个并不陌生的词映入大家眼帘：工业自动化。“激光加工自动化技术”被广泛应用在汽车、船舶、电子、半导体等行业，自动化加工着实为提高量产、减少人工、减少损耗做出了巨大的贡献。

不仅如此，“工业激光加工机器人”的应用范围也越来越广泛，其标准化、模块化、网络化和智能化程度越来越高，功能也越发强大。汽车、电子电器、工程机械等行业大量使用工业机器人自动化生产线，不仅节约了人工成本，而且能够确保产品质量和生产效率。

慕尼黑上海光博会的激光生产与加工技术展区，经过多年的打造和培育，已经成为中国乃至亚洲最具规模和影响力的激光加工品牌展，近年来，ABB 、REIS 、KUKA 、史陶比尔 、新松机器人等自动化工业企业的加盟，更大大增加展会的亮点。通快 、罗芬 、大族 、楚天 、华工 、金运 、泰德 、山东能源等领军企业的鼎力支持，将再次为 2014 年 3 月的展会带来行业内的集聚效应。